Mammoth Casa Diablo IV: A Case Study for Cooperative Baseline Analysis to Mitigate Environmental Impacts

John Akerley, Mark Hanneman, John Murphy, Adam Johnson, Drew Spake, Erica Freese, Derek Caro, Danny Feucht, Lu Lee

Ormat Technologies, Inc., Reno NV

Keywords

Casa Diablo, groundwater monitoring, case study, Long Valley, Mammoth, cooperative monitoring

ABSTRACT

The Mammoth Geothermal Complex has been in operation since 1984, and during this timeframe it underwent several expansions and repowers prior to the 2022 commissioning of the Casa Diablo IV station (CDIV). Due to its proximity to population centers, groundwater wells, hot springs, and thermal creeks, a fit-for-purpose monitoring network was installed ahead of field expansion to understand potential environmental impacts. Ormat cooperated with the Bureau of Land Management, the U.S. Forest Service, the U.S. Geological Survey, and the Mammoth Community Water District to collect and analyze baseline data prior to drilling new production and injection wells to support the CDIV project. During the CDIV commissioning, this monitoring network was reviewed as output from the new geothermal production wells was ramped up in incremental steps over a four-week period. The combination of strategic downhole pressure monitoring, geochemical monitoring, temperature monitoring, and ground leveling provided confidence that there would be no measurable impacts to nearby water resources, including thermal features and municipal water supply wells from CDIV operations. Now two years into operation, the water monitoring network continues, and no impacts have been identified.

1. Introduction

Ormat operates four binary geothermal power plants located about three miles east of the town of Mammoth Lakes, California and near the Casa Diablo hot springs. The binary cycle works by using hot geothermal fluid to vaporize a secondary working fluid like isobutane, which then powers a turbine. This process not only allows an efficient extraction of energy from the lower temperature geothermal resource compared to the steam turbine design but also allows 100 percent reinjection of geothermal brine. The first power plant at the site (G-1) began operating in 1985. Binary plants G-2 and G-3 were constructed in the early 1990s. In 2022, the fourth unit, the 30

megawatt (MW) Casa Diablo IV (CDIV) binary unit began commercial operation, bringing total production to 65 MW. Figure 1 shows the total production history of the Casa Diablo/Mammoth complex from 1985 to present, highlighting periods of increase in the early 1990s with expansion of two additional binary units and again in 2022 with the CDIV expansion. Throughout this timeframe, the total thermal-water discharge into Hot Creek, located east of the geothermal operations, has not changed (Evans et al, 2018).

Exploration drilling by the United States Geologic Survey (USGS), Ormat and others determined that the geothermal system's source area was west of the original Casa Diablo development in an area known as Basalt Canyon. Deeper wells drilled in the area in 2006 (57-25 and 66-25) were higher enthalpy (up to 375° F) than the lower Casa Diablo producers, highly permeable, and hydraulically connected to the Casa Diablo area. Further drilling at the western end of Basalt Canyon in 2010 (wells 12-25 and 14-25) also encountered the resource, leading to project release of CDIV.

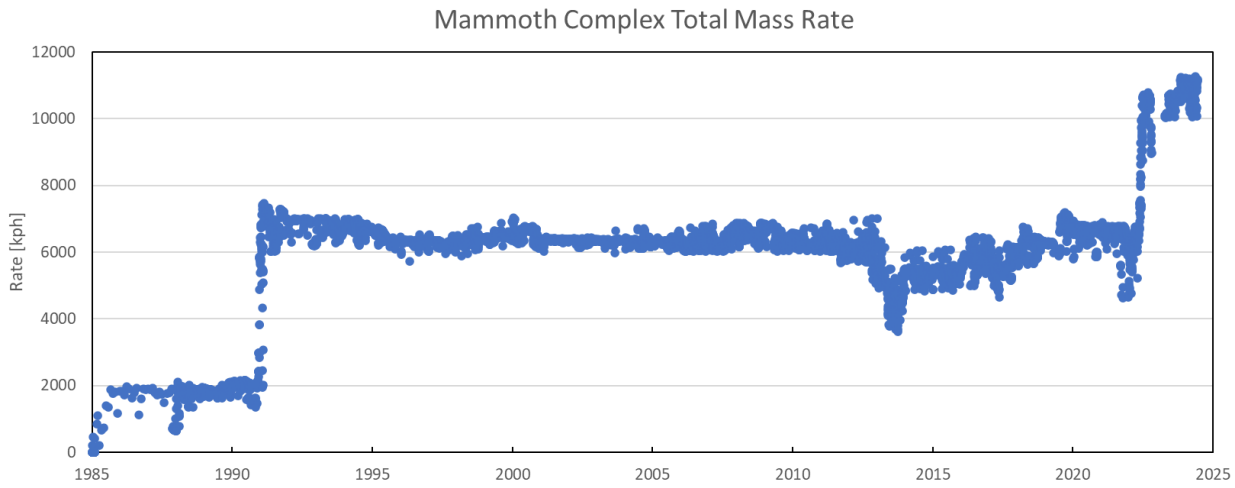

Figure 1: Total mass rate from the Mammoth geothermal complex since installation of the first binary unit in 1985 through June 2024. Flow unit is thousands of pounds per hour (kph).

A combined Environmental Impact Statement/Environmental Impact Report (EIS/EIR) was completed in 2013 that evaluated the potential impacts from CDIV development. All of the new production well sites were to be located in Basalt Canyon, closer to the town of Mammoth Lakes and to municipal water supply wells operated by the Mammoth Community Water District (MCWD). Since the community relies on these wells for drinking water and there are many stakeholders near the development, a special emphasis was placed on assessing potential impacts to that groundwater resource. Although geologic and hydrologic modeling indicated that the two systems were hydraulically disconnected and that impacts would not occur, it was decided that a fit-for-purpose groundwater monitoring and mitigation program would be implemented prior to initiating production in order to ease concerns around the development.

The CDIV Geothermal Development Project, Groundwater Monitoring and Response Plan (GMRP) was developed cooperatively by the BLM, Ormat, USGS, MCWD and the other agencies and finalized in January 2018. The purpose of this GMRP was to *"establish a monitoring program to detect any direct or indirect effects on the municipal water supply for the Town of Mammoth*

Lakes that may occur from geothermal production and injection associated with the CD-IV Project."

The objectives of the GMRP were to:

1) Identify and implement shallow groundwater aquifer, surface water resource, and deep geothermal reservoir monitoring strategies and protocols necessary to achieve this purpose, and

2) Establish a framework for determining and implementing appropriate response actions if, and when, needed to avoid, minimize, and/or mitigate potential adverse effects to the Town of Mammoth Lakes municipal water supply based on review and analysis of the monitoring data collected.

To meet these objectives, the GMRP outlined: 1) monitoring strategies, 2) data management, data reporting and plan evaluation strategies, and 3) response action strategies.

The GMRP is a cooperative, adaptive effort. An adaptive management approach was preferred because the committee recognized that hydrologic systems are dynamic and many factors can impact groundwater quality and quantity outside of geothermal production including climate, annual precipitation and its effect on aquifer recharge, variable groundwater production, regional seismic activity, and other natural source areas of geothermal fluid. As data is collected and analyzed, the monitoring strategy is reassessed, and new or refined approaches, methods or frequency are developed or optimized to ensure that the plan remains effective and practicable.

2. Geologic Setting

The Casa Diablo geothermal resource is present within a large volcanic feature known as the Long Valley Caldera. The geology of the caldera and the geothermal resources have been extensively studied and described over the past 35 years by Hildreth (2004, 2014, 2017), Bailey (1976), Sorey (1985, 1991, 1998), Suemnicht (1988), Evans (2017), and others. The following briefly summarizes these reports.

2.1 The Geothermal Resource

The geothermal resource wraps around the south and southwest margin of the resurgent dome in a hydraulically interconnected, highly-permeable zone of fractured welded tuffs belonging to two main units known as the Early Rhyolite and the underlying Bishop Tuff. The system's source area is believed to originate at great depth north of the town of Mammoth Lakes and near the Inyo Craters, another 3.5 miles northwest of Basalt Canyon. Due to difficult terrain and the depth needed to reach the resource, few wells have been drilled west of Basalt Canyon, so the exact source area remains uncertain. Figure 2 shows the regional geology and resurgent dome from Hildreth (2017).

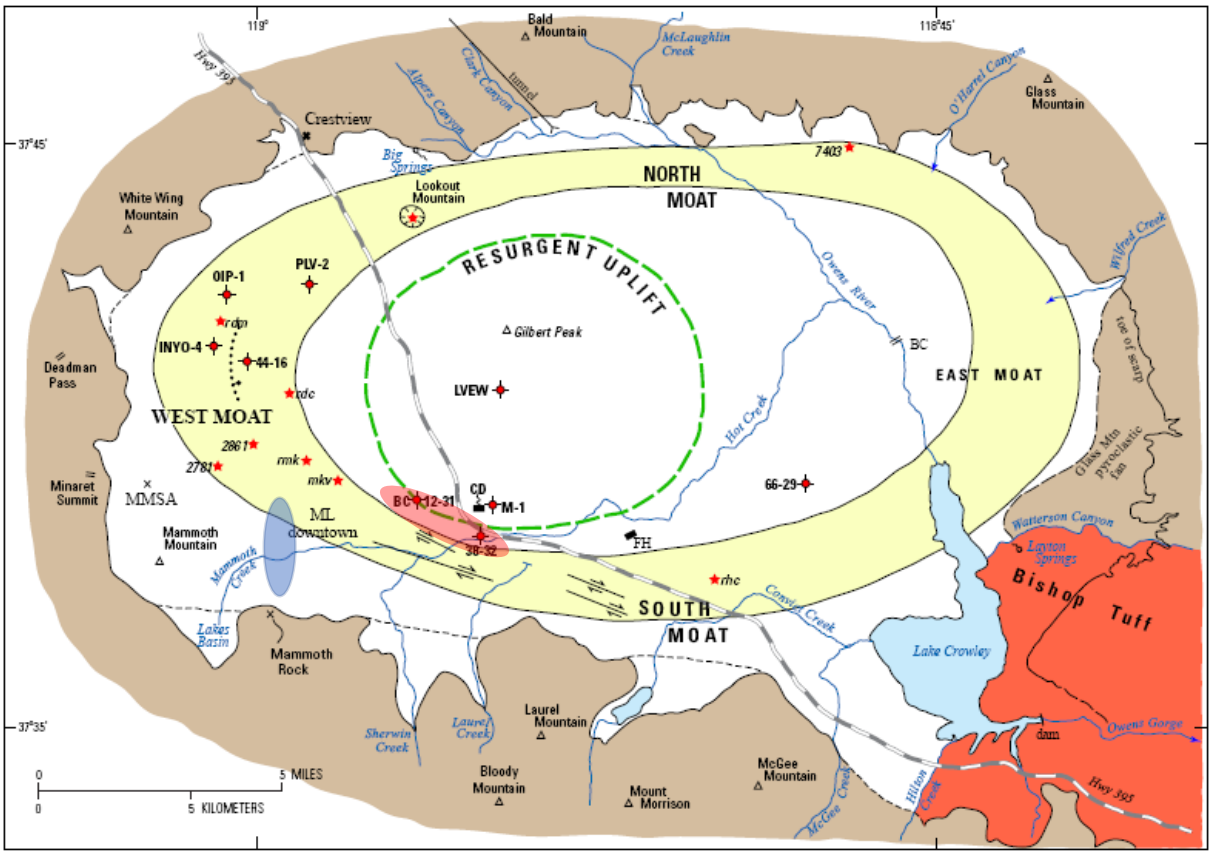

Figure 2: Figure from Hildreth (2017). The resurgent dome is comprised of Early Rhyolite, while basalt flows infill the south and west moat. General location of Ormat geothermal wells highlighted in the red oval, and groundwater municipal wells highlighted in blue oval. Legend: structural ring-fault zone (yell), Precaldera rocks (brown), Bishop Tuff ignimbrite outflow (red), dashed lines crossing caldera-wall embayments suggest continuity of basement rocks concealed beneath modern surficial deposits.

The geothermal production wells in Basalt Canyon include 57-25 and 66-25 drilled in 2005; 14-25 in 2010; 12-25 in 2011; and 47-25 (drilled next to 57-25), 14B-25 and 14C-25 (both drilled adjacent to 14-25) drilled in 2022. The wells have been drilled right up to the eastern edge of the West Moat Coulee where the system was first encountered in wells 14-25 and 12-25.

The system flows eastward through Basalt Canyon, beyond Casa Diablo, to Hot Creek where it ultimately discharges to the surface in a series of hot springs. Total system flow is reportedly 370 kg/s (about 5,500 gpm) at 220° C. The system has a relatively flat horizontal gradient due to its high permeability. In Basalt Canyon, the static water level in the production wells is about 450 feet below the surface and within the Early Rhyolite tuffs. As topography drops from west to east, the water level slowly approaches the land surface, until the system discharges into Hot Creek several miles east of Casa Diablo.

Basalt Canyon wells typically encounter high enthalpy fluids at a depth of about 1,000 ft in a moderately permeable zone in the Early Rhyolite. Below this is a thick section of tuff breccias, and clastic/lacustrine sediments and conglomerates that are essentially impermeable. These materials are underlain by the Bishop Tuff. Total lost circulation in the Bishop Tuff is limited to specific fractured zones, and is encountered at depths ranging from 1600 to 2100 ft. This lower

zone is highly productive but is generally cooler than the upper zone in the Early Rhyolite. The high permeability is likely a combination of open fractures along steep faults passing through brittle welded tuffs, and possibly along undetermined horizontal surfaces on top of individual welded tuff layers.

Cooled fluids from all production wells are reinjected into the deep Bishop Tuff at Casa Diablo near the G-2 and G-3 power plants. Injection wells 54A-32 and 54B-32 were drilled in 2021 for CDIV. There is little communication of this deep injection with the overlying production wells in the Early Rhyolite, but tracer studies in 1992, 2017, and 2023 have shown eventual migration of injection in Bishop Tuff to the Lower Casa Diablo producers.

The resource is bounded on the south by the ring fault zone which places down-dropped moat basalts against the Early Rhyolite. Geophysics indicates that the rings faults likely underlie Highway 203; however, the fault zone is entirely covered by till and younger basalt flows and is nowhere exposed, nor has it been intercepted by drilling. The mag low may be partially masked by basalt flows north of Highway 203.

A few test wells drilled south of Basalt Canyon within the moat and into the underlying Early Rhyolite have not encountered temperatures greater than 175°F. Magnetic surveys indicate that the resurgent dome forms the northern boundary to the system, but that it extends northward somewhat along the NNW-trending faults (see Figure 3). Hydrothermal alteration and small fumaroles locally extend to the surface along these faults in the vicinity of the known resource.

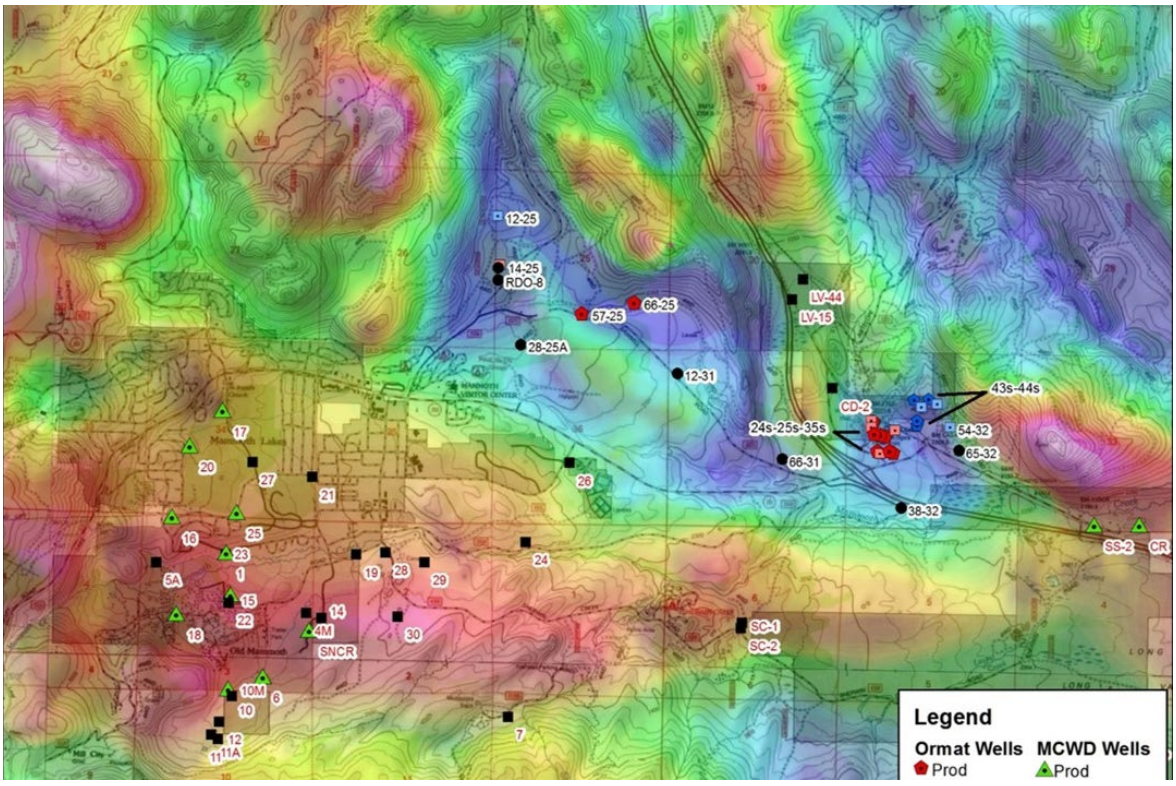

Figure 3: Location of municipal groundwater wells and geothermal wells. Background shading is natural magnetic field intensity from an aeromagnetic survey. Areas of low magnetic intensity (blue shading) map hydrothermal alteration associated with the geothermal system.

2.2 The Groundwater Resource

The municipal groundwater resource is located in the southwest moat and on the east flank of Mammoth Mountain (see Figure 2). Groundwater is produced from nine wells that are oriented in a north-south alignment. All groundwater production wells are located 1.8 miles or more from the closest Basalt Canyon geothermal production well.

The aquifer is hosted by an approximately 1,000-ft-thick sequence of mafic volcanic lavas and cinders that originated from the base of Mammoth Mountain west of the wells. Interflow glacial till is present in some wells. The aquifer is largely recharged by snowmelt and infiltration from Mammoth Creek and Mammoth Mountain. Numerous exploratory wells drilled east of the production wells within the moat had low productivity (Schmidt et al 2018).

The groundwater wells are about 700 ft deep and moderately productive. Water levels decline as pumping increases, but at variable rates due to widely varying transmissivities. Well P17 is the most productive and produces about 800 gpm with about 4 feet of drawdown. Annual operational summaries for all wells are available on the MCWD website.

Four of the wells regularly exceed the arsenic drinking water standard of 10 µg/L; three of the wells occasionally exceed the standard, and two of the wells do not exceed the standard. Well P17 water, on the north end of the field, typically contains between 86 and 150 µg/L arsenic (As). Several wells also exceed the secondary drinking water standard for iron (0.3 mg/L) and manganese (0.05 mg/L). Water temperature is highest in northern and western wells, and generally increases with increasing production and declining water levels. Well P17 is the warmest (up to 81° F), see Figure 4 for location of P17 with respect to geothermal system.

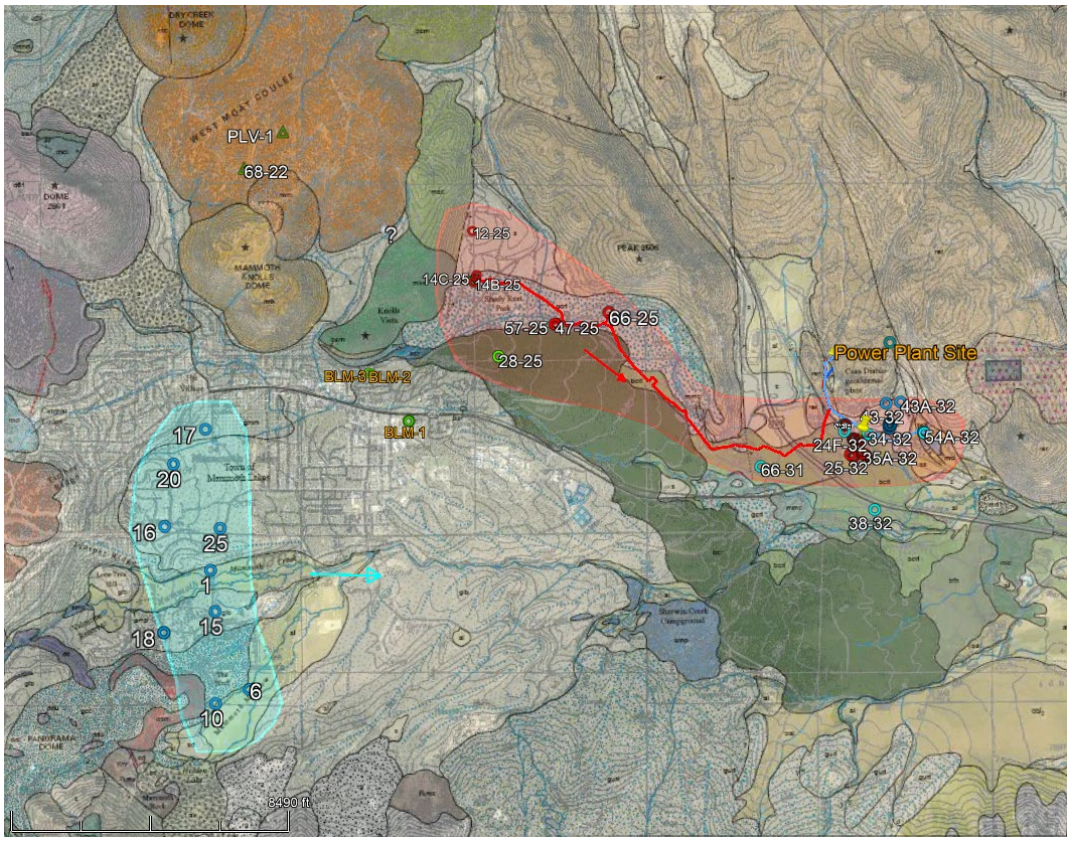

Figure 4: Geologic map showing location of MCWD (blue) and geothermal system (red). Well 17 is closest to geothermal source area and produces water containing elevated temperature and metals.

Chloride is a conservative element that is not normally present in area groundwater but is present in the geothermal fluid. As a result, it has been used to estimate that in P17, which contains the most chloride of the groundwater producers, contains about 2-3% geothermal fluid. Chloride in that well reached an all-time high of about 12 mg/L in late 2016 following three years of drought and regular production pumping. However, melting and infiltration of the large snowpack in the spring of 2017 resulted in significant recharge to the groundwater aquifer that returned chloride concentrations to lower levels by early 2020. Figure 5 shows the chloride trends for seven of the groundwater production wells including this P17 trend. Concentrations again increased during the 2020-2022 drought years. Since geothermal operations were constant during this period (see Figure 1), these responses indicate that the arsenic and chloride content in the groundwater supply wells is unrelated to the Mammoth geothermal complex operations.

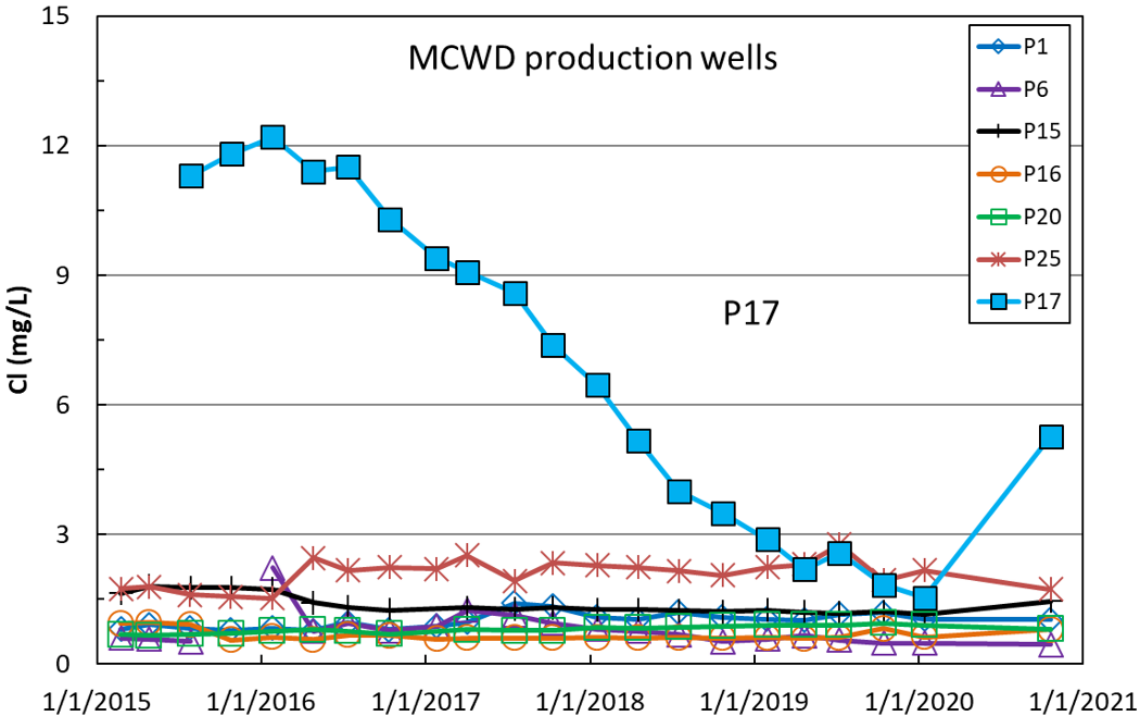

Figure 5: Groundwater production geochemistry chloride (Cl) trends from 2015 to 2021. Note decrease in sampling frequency in 2020 due to Covid-19 restrictions.

3. Monitoring Well Network

The GMRP established a baseline monitoring well network comprised of 28 sites that included a combination of shallow groundwater, dual completion (shallow and intermediate depth), and geothermal reservoir wells to be monitored for temperature, pressure/water level, and geochemical parameters, depending on well type. Tables 2 and 3 outline the types of data collected.

Since 2015, the BLM in coordination with the US Forest Service (USFS), the USGS and MCWD, has approved the installation of several wells dedicated to the CDIV Project. Table 1 summarizes the well constructions.

- 14A-25 is a 600-ft-deep, dual completion monitoring well installed by the USGS in 2015. 14A-25 is located on the well pad that hosts production wells 14B-25 and 14C-25, and standby production well 14-25. 14A-25 monitors fluid in the Early Rhyolite about 400 ft above the upper production zone.
- 28A-25 is a 600-ft-deep, dual completion monitoring well installed by the USGS in 2015. The well is 2,000 feet southwest of production wells 47-25 and 57-25, but still 1.75 miles down-gradient of the closest MCWD well. Both monitoring point are constructed in the Early Rhyolite.
- 28-25 is located next to 28A-25 and is a 1622 ft deep core hole installed by Ormat in 2017. The well measures pressure within the Bishop Tuff.

- BLM-1 is a dual completion monitoring well drilled to 600 ft by USGS in 2017. The well is completed in the moat basalts.
- BLM-2 is a 680-ft-deep dual completion monitoring well drilled by USGS in 2021 to monitor a hypothetical fault running between the MCWD wells and Basalt Canyon. Both wells are completed in the Early Rhyolite.
- BLM-3 is a 1320-ft-deep well installed by USGS in 2021, ostensibly to monitor the Bishop Tuff in a theoretical fault running between the groundwater wells and Basalt Canyon. The well, however, was completed in Early Rhyolite.

The groundwater production well group includes MCWD wells 1, 6, 15, 16, 17, 20, and 25.

Table 1. Monitoring Well Construction Summary (bolded wells indicate Moat basalts vs. Early Rhyolite completion).

Well Number	Installed by	Screen Interval	Filter Pack Interval	Geology of screened interval
14A-25 Shallow	USGS	470-490	446-496	Rhyolite tuff and obsidian. Base of basalt at 196 ft.
14A-25 Deep		575-595	555-600	Altered rhyolite tuff
28A-25 Shallow	USGS	440-460	418-481	Rhyolite xtl tuff
28A-25 Deep		575-595	555-602	USGS incorrectly logged as andesite. Core from adjacent well 28-25, has vuggy, pumiceous, pinkish grey rhyolite at this depth.
28-25	Ormat	Cased to 1322'. Slotted 1407 to 1622'		Monitors pressure in the geothermal reservoir. Bishop Tuff present from 1524ft to bottom. Total loss of circulation at 1620 ft. USGS sinker bar stuck at 1440ft.
BLM-1 Shallow	USGS	415-435	395-455	Vesicular basalt.
BLM-1 Deep		520-540	488-541	Vesicular basalt
BLM-2 Shallow	USGS	440-460	420-480	Early Rhyolite. Well construction uncertain. Base of basalt isat 408'
BLM-2 Deep		640-660	620-680	Early Rhyolite. Base of basalt at 408 ft
BLM-3 Deep	USGS	1190-1300	1180-1320	Early Rhyolite. Base of basalt at 404 ft. Well is screened in Early Rhyolite.
MW-33	USGS for MCWD	610		Basalt

3.1 Monitoring and Sampling Requirements

Table 2 outlines the baseline monitoring well network, including the type of well (target formation) as well as the parameters and frequency of data collection for the wells within the GMRP program.

Table 3 outlines the geochemical constituents that are analyzed at the frequency specified under the "Geochemical" column in Table 2.

Table 2. Baseline monitoring well network and parameters

Well Type	Well Name	Monitoring Entity	Temperature	Pressure	Water Level	Geochemical
Shallow Groundwater Monitoring Wells	MCWD 14	MCWD			D (t)	
	MCWD 19				D (m)	
	MCWD 24				D (t)	
	MCWD 26	MCWD & USGS	D (t)		D (t)	Q
	SC-1	Ormat & USGS	D (t)		D (t)	
	SC-2		D (t)		D (t)	
Shallow Groundwater Production Wells	MCWD 1	MCWD & USGS			D (t)	Q
	MCWD 6				D (t)	Q
	MCWD 15				D (t)	Q
	MCWD 16				D (t)	Q
	MCWD 17				D (t)	Q
	MCWD 18				D (t)	
	MCWD 20				D (t)	Q
	MCWD 25				D (t)	Q
Dual Completion Monitoring Wells	14A-25-Shallow [490 feet] and 14A-25-Deep [595 feet])	USGS	Q (VTP)	D (b)		Q
	28A-25-Shallow [460 Feet] and 28A-25-Deep [595 feet]		Q (VTP)	D (b)		Q
	BLM-1-Shallow [435] and BLM-1-Deep [580]		Q (VTP)	D (b)		Q
Geothermal Reservoir Monitoring Wells	Ormat 12-31	Ormat	D (b)	D (b)		
	Ormat 65-32		D (b)	D (b)		
	Ormat 48-29		D (t)	D (t)		
	Ormat 28-34		D (b)	D (b)		
	Ormat CW-3		D (t)	D (t)		
	USGS CH10B	USGS		D (b)		
	Ormat 28-25		Q (VTP)	D (b)		Q
	BLM Off-Lease 2		Q (VTP)	D (b)		Q
Geothermal Reservoir Production Wells	Ormat 57-25	Ormat & USGS	D (b)	D (b)		Q
	Ormat 66-25		D (b)	D (b)		Q
	Ormat 12-252	Ormat	TBD	D (b)		TBD
	Ormat 14-252		TBD	D (b)		TBD

Notes: D = Daily Average, Q = Quarterly, TBD = To Be Determined, (t) = Transducer, (b) = Bubbler Tube, (m) = Manual, VTP = Vertical Temperature Profile

Table 3. Constituents and parameters in monitoring program

Constituents and Parameters	Units
Chemicals and Parameters	
Alkalinity - Field	Milligrams per liter (mg/l) Field Raw Water Alkalinity
Acid Neutralizing Capacity (ANC)	Milligrams per liter (mg/l)
Arsenic (As)	micrograms per liter (µg/l)
Boron (B)	micrograms per liter (µg/l)
Bromide (Br)	micrograms per liter (µg/l)
Calcium (Ca)	milligrams per liter (mg/l)
Chloride (Cl)	milligrams per liter (mg/l)l
Fluoride (F)	milligrams per liter (mg/l)l
Lithium (Li)	micrograms per liter (µg/l)
Magnesium (Mg)	milligrams per liter (mg/l)
Nitrogen, ammonia (NH_3) as N	milligrams per liter (mg/l)
Nitrogen, as nitrite (NO_3)	milligrams per liter (mg/l)
pH	pH units
pH	pH units
PO_4	milligrams per liter (mg/l)
Potassium (K)	milligrams per liter (mg/l)
Total Dissolved Solids (TDS)[2]	milligrams per liter (mg/l)
Rubidium (Rb)[1]	micrograms per liter (µg/l)
Silica (Si)	milligrams per liter (mg/l)
Sodium (Na)	milligrams per liter (mg/l)
Specific conductance	microseimens per centimeter (µS/cm)
Specific conductance	microseimens per centimeter (µS/cm)
Sulfate (SO_4)	milligrams per liter (mg/l)
Temperature	°C
Temperature	°C
Non-Condensable/Dissolved Gases	
H_2S[1]	
Isotopes	
D/H ratio (Deuterium/Hydrogen)	per mil
$^{18}O/^{16}O$ ratio	per mil
Tritium (^3H)[1]	One-time sample of 14A-25, 28A-25, MCWD 26, and other select MCWD production wells (TBD) to establish existing concentrations; then, annual sampling from select geothermal production wells in Basalt Canyon (TBD); Data not yet available
Additional Constituents and Parameters	Consistent with the adaptive monitoring framework of the GMRP, additional constituents and parameters may be added for specific tests or to improve monitoring effectiveness based on new information

Notes:

[1] H_2S, rubidium, and tritium not yet incorporated into field sampling program.

[2] Laboratory calls total dissolved solids "residue."

4. Mammoth CDIV Stress Test Summary

Prior to full-time facility operations, a production stress test was performed on the new Basalt Canyon wells to demonstrate that CDIV operations would not impact groundwater wells. Data from monitoring wells 14A-25, 28-25 shallow, 28-25 Deep, BLM 1, and BLM 2 were monitored during the test for changes in water level. Four production steps, or test phases, were completed during the testing. Data from each phase was presented to the GMRP committee comprised of Ormat, BLM, MCWD, and the USGS for their review and approval prior to advancing to the next phase. Approval criteria related to the quality of data as well as the change, or lack thereof, in the water levels for each lithology.

This stress test, while instrumental in validating the environmental safety of the geothermal operations, represents a high level of scrutiny that may not be universally applicable or necessary for all geothermal projects. It is recommended that the deployment of such stress tests be considered on a case-by-case basis, taking into account the unique geological, hydrological, and ecological characteristics of each site as well as the size of the geothermal project. For projects in areas with lower sensitivity or established historical data demonstrating minimal risk, a scaled-down version of the stress test or alternative monitoring methods may be more appropriate. This approach ensures that resources are allocated efficiently, focusing intensive testing methods like those used in for CDIV on developments where the potential for environmental impact is greatest.

A full list of activities detailing the four phases of the test are outlined in Table 4. Figures 6 through 11 show the responses in the shallow monitoring wells 14A-25, 28A-25, BLM 1, and BLM 2 during the various phases. These monitoring wells show a primary response to atmospheric pressure conditions and minor, basin-wide water level decline during the summer months. Shallow well 14A-25 is located between production wells 14B-25 and 14C-25 and is constructed in hot Early Rhyolite. The USGS determined that the well exhibits poro-elastic effects on the order of less than 0.5 feet (0.2 psi) during startups of those production wells (Howle 2020). This response was also observed during the 2017 long-term flow test.

Monitoring well 28-25 Deep is completed in the Bishop Tuff geothermal reservoir and shows a direct varying response of drawdown as expected from the increase in flow. 28-25 deep also clearly displays pressure recovery equal to prior state during periods of lesser flow. Table 4 shows various events and dates which occurred during the duration of the test. Table 5 shows the change in depth of water level in ft for 14A-25, 28-25 shallow, 28-25 Deep, BLM 1, and BLM 2. Figure 12 shows the location of production and monitoring wells.

The CDIV stress test was completed in July 2022 after 6 weeks of flow variation and monitoring data analysis.

Table 4. List of events during the 2022 CDIV stress test

Date	Event
5/19/2022	47-25 Online
5/27/2022	14C-25 Online
6/1/2022	14C-25 offline and 47-25 online
6/2/2022	14C-25 at full capacity and 47-25 online at reduced capacity **(Phase 1)**
6/3/2022	47-25 online at full capacity; total flow ~5000 gpm
6/4/2022	All wells online, total flow ~5000 gpm
6/6/2022	Only 47-25 online
6/11/2022	All wells online, total flow ~6500 gpm (Nominal flow: **Phase 2**)
6/13/2022	All wells online, total flow ~7000 gpm (Nominal flow)
6/16/2022	CDIV down for 0.5 hours. CDIV unit started at 06:03. Test Energy/Commissioning.
6/17/2022	CDIV down for 2.3 hours. Unit started at 13:27.
6/22/2022	All wells online, total flow ~6000 gpm
6/24/2022	All wells online, total flow ~8400 gpm
6/25/2022	Flow reduced to 4000-4500gpm (50 % of full capacity) (**Phase 3**)
6/28/2022	CDIV down 10 hours. Unit online at 16:25
6/29/2022	Total flow 8700 gpm (**Full capacity**)
6/30/2022	Total flow 8700 gpm (Full capacity)
7/1/2022	CDIV down 3.8 hours
7/6/2022	End of the stress test. Total flow 8700 gpm (Full capacity)

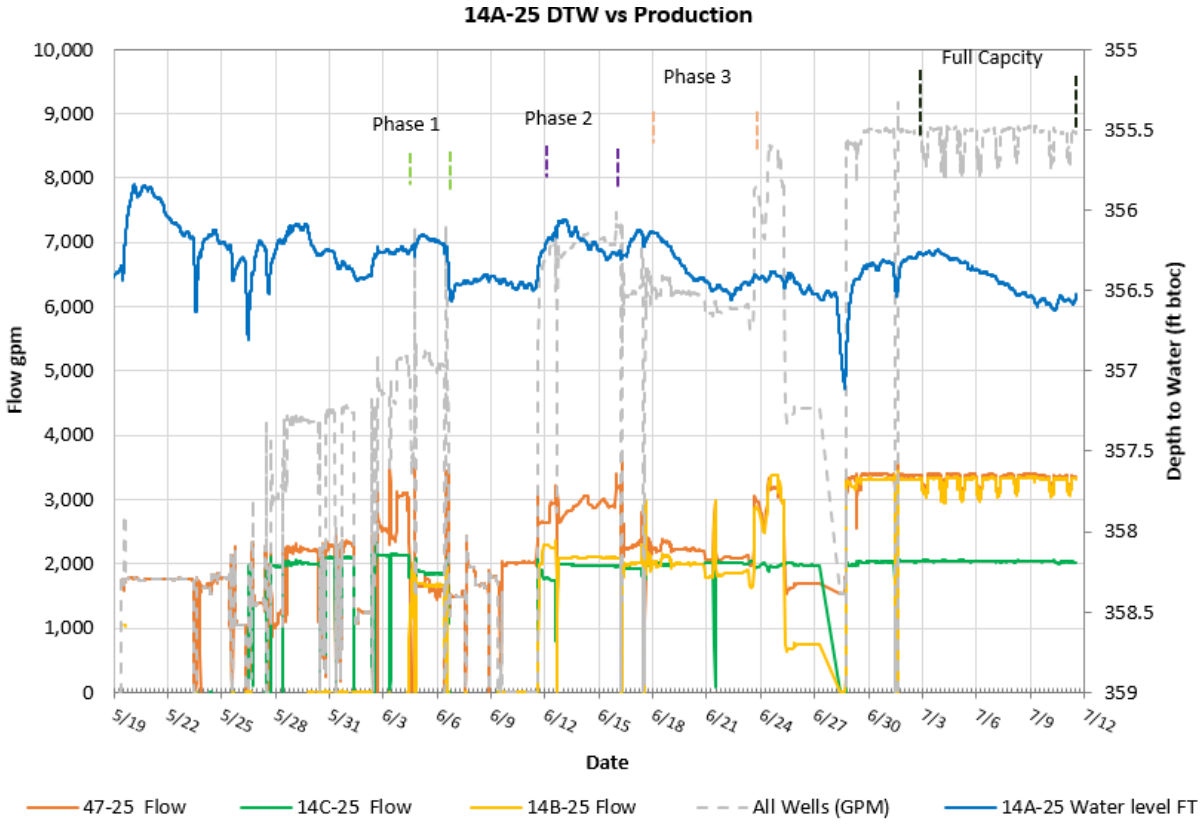

Figure 6: 14A-25 water level and CDIV production flow during four phases of stress test.

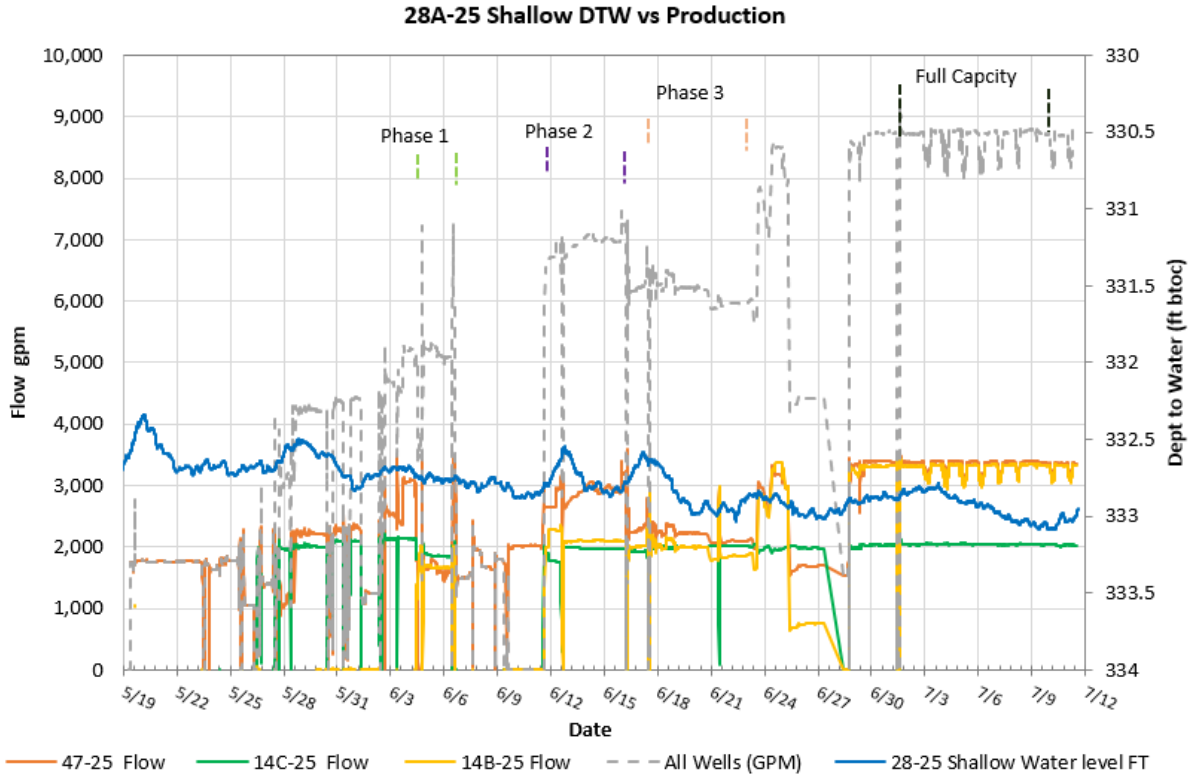

Figure 7: 28-25 Shallow water level and CDIV production flow during four phases of stress test.

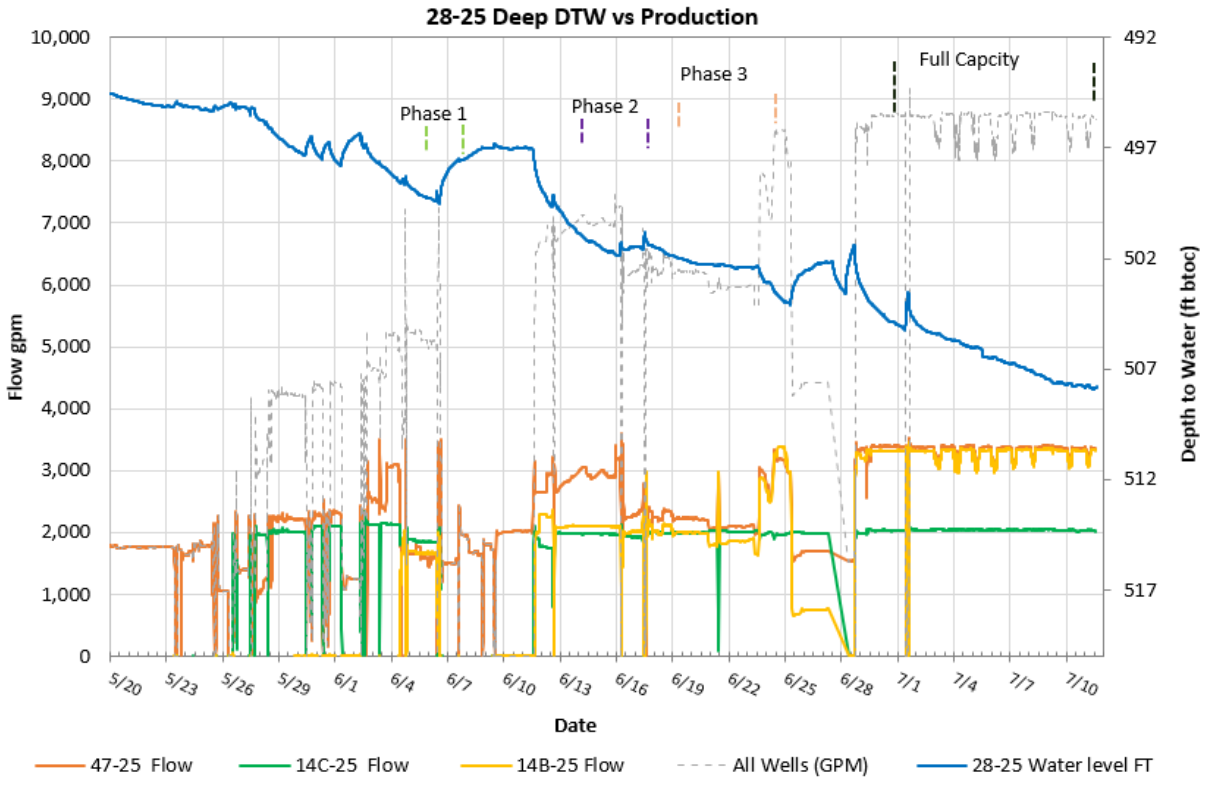

Figure 8: 28-25 Deep water level and CDIV production flow during four phases of stress test.

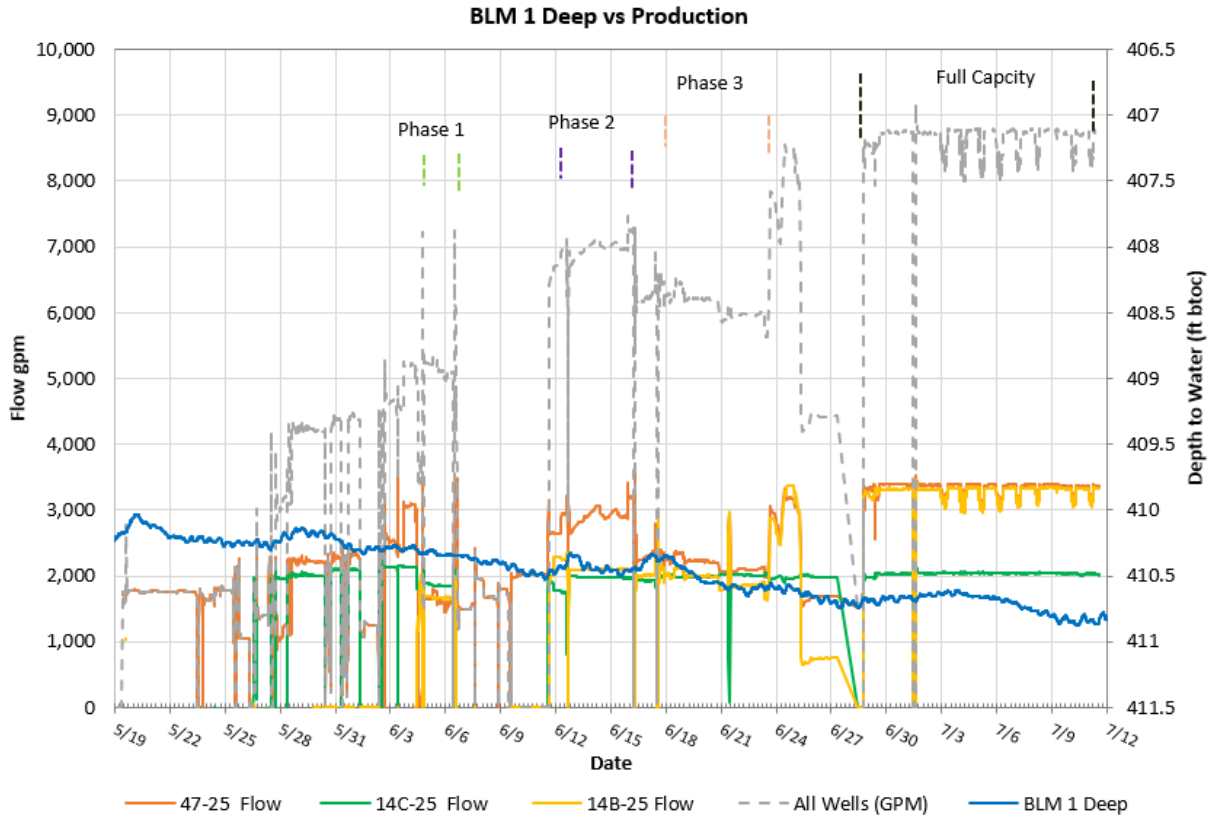

Figure 9: BLM 1 Deep water level and CDIV production flow during four phases of stress test.

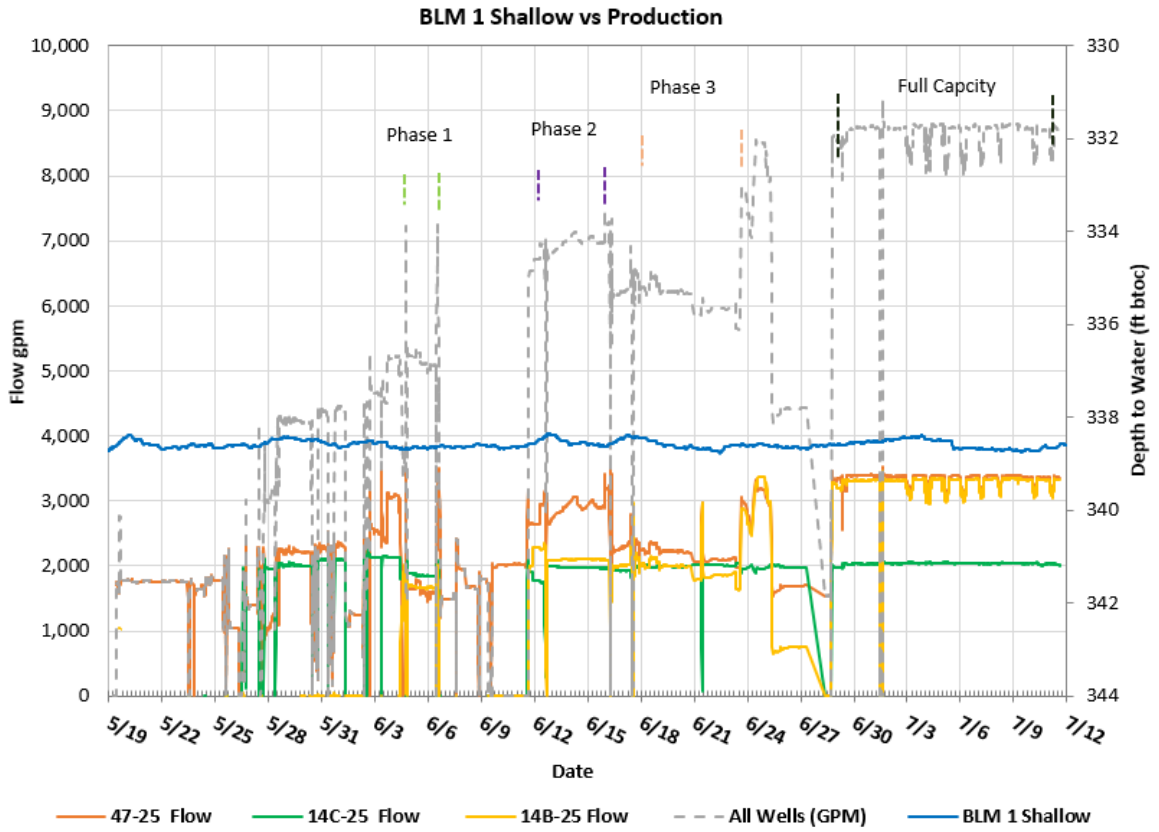

Figure 10: BLM 1 Shallow water level and CDIV production flow during four phases of stress test.

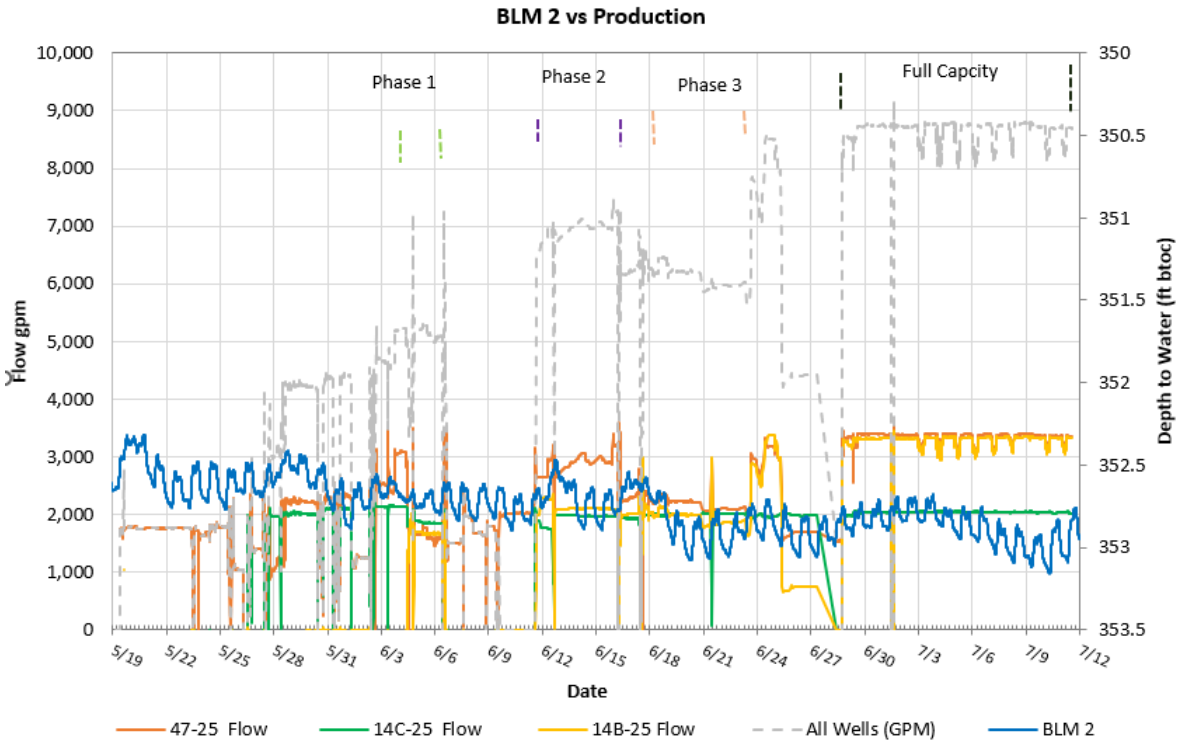

Figure 11: BLM 2 water level and CDIV production flow during four phases of stress test.

Table 5. Depth (ft) to water levels from ground surface before and after the Stress test in each monitoring well. Positive difference indicates a drop in water level.

Depth to Water Level from Ground Surface (ft)						
Date	**Well**					
	14-25	**28-25 shallow**	**28-25 Deep**	**BLM 1 Deep**	**BLM 1 Shallow**	**BLM 2**
5/19/2022 (CDIV Production Flow : 0 gpm)	356.38	332.40	494.53	410.11	338.46	352.37
7/11/2022 (CDIV Production Flow : 8800 gpm)	356.52	332.95	507.82	410.85	338.61	352.93
Difference:	-0.14	0.55	13.29	0.74	0.15	0.56

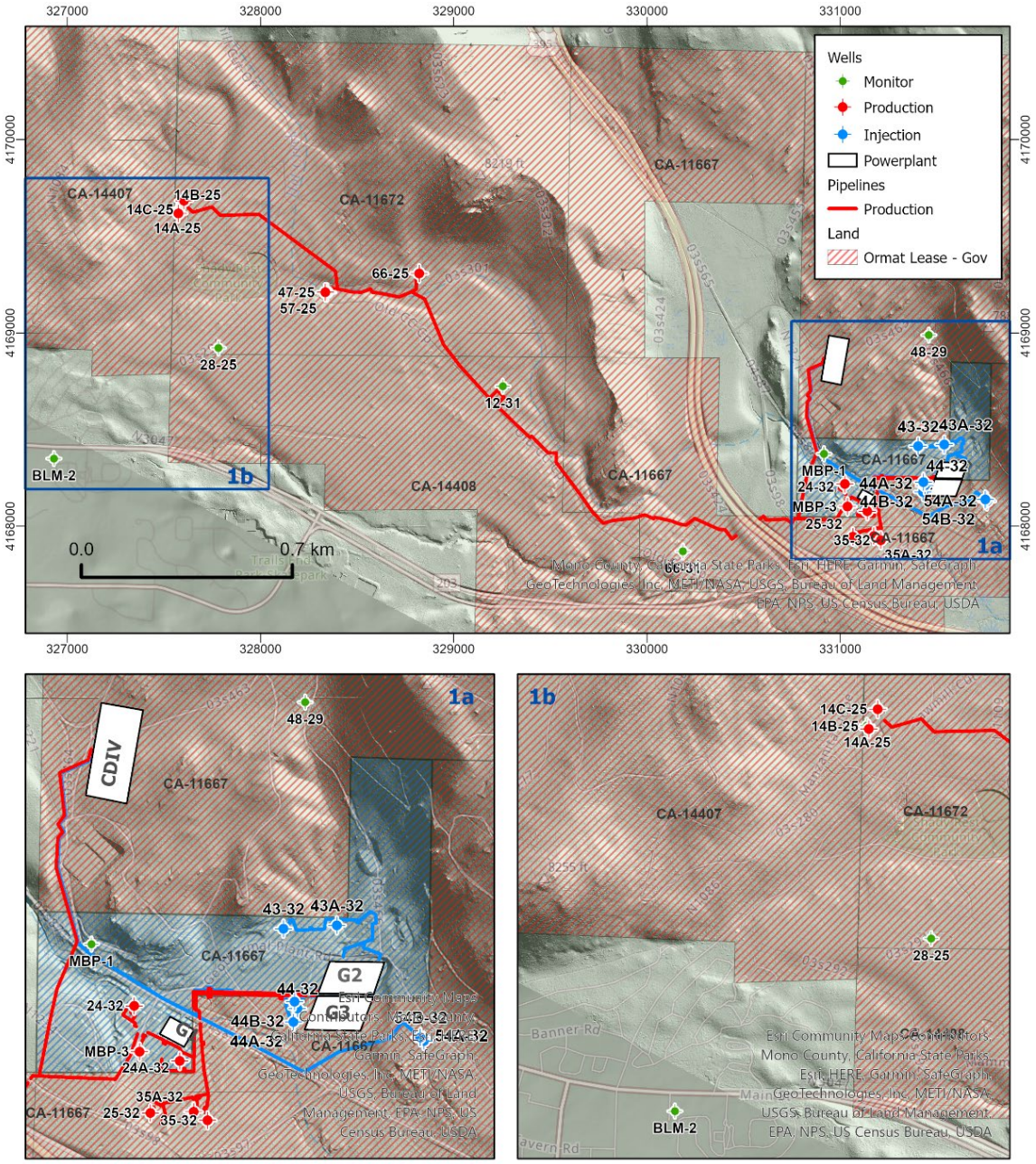

Figure 12: Map showing location of Ormat production (red) and injection (blue) wells along with select monitoring wells (green).

5. Conclusions

Water quality issues, including elevated arsenic, existed in several municipal water production wells that appeared to be of geothermal origin. Previous geologic, hydrologic, and geochemical data indicated that the Basalt Canyon geothermal reservoir and the groundwater aquifer were hydraulically disconnected systems hosted in different rock formations. Because the specific source of the contaminants in these municipal water supply wells had never been identified, some

agencies were still concerned that they were related to Mammoth complex geothermal operations. To allay these concerns and to provide an early warning system should any unforeseen impacts occur, an adaptive but rigorous GMRP was cooperatively developed by Ormat and local, State and Federal agencies. The GMRP was enacted prior to and during startup of the new CDIV production wells.

The monitoring program included a network of shallow groundwater wells, intermediate depth wells, and deep reservoir wells instrumented to track water levels, temperatures, and geochemical parameters. Baseline data were collected for several years leading up to CDIV operations. Once the new production wells were drilled, a carefully designed step-rate stress test was conducted, incrementally increasing flow from the wells while closely monitoring the well network. As expected, the deep monitoring wells within the geothermal reservoir showed a direct response to the changing reservoir pressure during flow variations, but corresponding signals were not observed in either the shallow groundwater monitoring array near the geothermal system or in the municipal water supply wells.

It's important to note that the monitoring program outlined in this case study, while successful in evaluating potential environmental impacts for this development, represents an extensive undertaking that may be prohibitive for geothermal projects in early development or smaller in size. The level of baseline data collection, multi-agency cooperation, and ongoing monitoring was warranted given the proximity to the municipal water supply for Mammoth Lakes and the size of the geothermal project. However, a more streamlined process may be suitable for geothermal developments in less environmentally-sensitive areas or where the risks of groundwater impacts are lower based on preliminary studies. An appropriate balance must be struck between environmental safeguards and enabling cost-effective geothermal energy development.

Now two years into full CDIV operations at a combined complex capacity of 65 MW, the monitoring program continues and has not detected any impacts to the groundwater system to-date, and discussions regarding appropriate reductions to components of the monitoring plan have begun. The cooperative monitoring effort successfully demonstrated that the expanded geothermal operations can be conducted safely without detriment to the community's water resources. The adaptive monitoring program will remain in place going forward to provide long-term tracking and response capability should any future changes occur. This case study highlights the value of establishing comprehensive environmental baselines and monitoring programs through interagency collaboration when developing renewable energy resources in environmentally sensitive areas.

REFERENCES

Bailey, R.A., Dalrymple, G.B., and Lanphere, M.A., 1976, Volcanism, structure, and geochronology of the Long Valley caldera, Mono County, California: Journal of Geophysical Research, v. 81, no. 5, p. 725–744, https://doi.org/10.1029/JB081i005p00725.

Bergfeld, D., Evans, W.C., Howle, J.F., and Farrar C.D., 2006, Carbon dioxide emissions from vegetation-kill zones around the resurgent dome of Long Valley Caldera, eastern California, USA: Journal of Volcanology and Geothermal Research, v. 152, no. 1–2, p. 140–156, https://doi.org/10.1016/j.jvolgeores.2005.11.003.

Bergfeld, D., Vaughan, R.G., Evans, W.C., and Olsen, E., 2015, Monitoring ground-surface heating during expansion of the Casa Diablo production well field at Mammoth Lakes, California: Geothermal Resources Council Transactions, v. 39, p. 1007–1013, https://www.geothermal-library.org/index.php?mode=pubs&action=view&record=1032246.

Brown, S.T., Kennedy, B.M., DePaolo, D.J., Hurwitz, S., and Evans, W.C., 2013, Ca, Sr, O and D isotope approach to defining the chemical evolution of hydrothermal fluids—Example from Long Valley, CA, USA: Geochimica et Cosmochimica Acta, v. 122, p. 209–225, https://doi.org/10.1016/j.gca.2013.08.011.

Bureau of Land Management, 2013, Record of Decision, Casa Diablo IV Geothermal Development Project, Case File Number: CACA 054722: Bishop, California, 19 p., https://openei.org/w/images/7/7c/CD-IV_Final_BLM_ROD_081213.pdf.

Bureau of Land Management, 2018, CD-IV Geothermal Development Project—Groundwater Monitoring and Response Plan, version 1.1 dated January 19, 2018, 29 p.

Evans, W.C., 2017, Overview of the Long Valley hydrothermal system after decades of study, in Hildreth, W., and Fierstein, J., 2017, Geologic field-trip guide to Long Valley Caldera, California: U.S. Geological Survey Scientific Investigations Report 2017–5022–L, p. 99–119, https://doi.org/10.3133/sir20175022L.

Evans, W.C., and Bergfeld, D., 2017, Groundwater resources of the Devils Postpile National Monument—Current conditions and future vulnerabilities: U.S. Geological Survey Scientific Investigations Report 2017–5048, 31 p., https://doi.org/10.3133/sir20175048.

Evans, W.C. et al, 2018, Hot Water in the Long Valley Caldera—The Benefits and Hazards of this Large Natural Resource. U.S. Geological Survey Fact Sheet 2018–3009, 4 p., https://doi.org/10.3133/fs20183009.

Farrar, C.D., Sorey, M.L., Roeloffs, E.R., Galloway, D.L., Howle, J.F., and Jacobsen, R., 2003, Inferences on the hydrothermal system beneath the resurgent dome in Long Valley Caldera, east-central California, USA, from pumping tests and geochemical sampling: Journal of Volcanology and Geothermal Research, v. 127, p. 305–328, https://doi.org/10.1016/S0377-0273(03)00174-4.

Farrar, C.D., DeAngelo, J., Williams, C.F., and Hurwitz, S., 2010, Temperature data from wells in Long Valley Caldera, California: U.S. Geological Survey Data Series 523, https://doi.org/10.3133/ds523.

Galloway, D.L., 2019, Atmospheric-loading frequency response functions and groundwater levels filtered for the effects of atmospheric loading and solid Earth tides for three monitoring wells near Mammoth Lakes, California, 2015–2017: U.S. Geological Survey data release, https://doi.org/10.5066/P9ON8U5U.

Hildreth, W., 2004, Volcanological perspectives on Long Valley, Mammoth Mountain, and Mono Craters—Several contiguous but discrete systems: Journal of Volcanology and Geothermal Research, v. 136, nos. 3–4, p. 169–198, https://doi.org/10.1016/j.jvolgeores.2004.05.019.

Hildreth, W., Fierstein, J., Champion, D., Calvert, A., 2014, Mammoth Mountain and its mafic periphery—A late Quaternary volcanic field in eastern California: Geosphere, v. 10, p. 1315–1365, https://doi.org/10.1130/GES01053.1.

Hildreth, W., Fierstein, J., Champion, D., Calvert, A., 2017, Early postcaldera rhyolite and structural resurgence at Long Valley Caldera, California. Journal of Volcanology and Geothermal Research, v. 335 p. 1-34, http://dx.doi.org/10.1016/j.jvolgeores.2017.01.005.

Hildreth, W., 2017, Fluid-driven uplift at Long Valley Caldera, California: Geologic perspectives. Journal of Volcanology and Geothermal Research, v. 341, p. 269–286, https://doi.org/10.1016/j.jvolgeores.2017.06.010.

Hildreth, W. and Fierstein, J., 2017, Geologic field-trip guide to Long Valley Caldera, California: U.S. Geological Survey Scientific Investigations Report 2017–5022–L, 119 p., https://doi.org/10.3133/sir20175120L

Hill, D.P., Bailey, R.A., and Ryall, A.S., 1985, Active tectonic and magmatic processes beneath Long Valley Caldera, eastern California—An overview: Journal of Geophysical Research, v. 90, no. B13, p. 11111–11120, https://doi.org/10.1029/JB090iB13p11111.

Howle, J.F., 2020. Long Valley Hydrologic Advisory Committee Hydrologic Monitoring Data Unpublished and provisional U.S. Geological Survey Data through December 2019 - Submitted by J.F. Howle. Prepared Jan 30, 2020. 25p.

Peacock, J.R., Mangan, M.T., McPhee, D., and Wannamaker, P.E., 2016, Three-dimensional electrical resistivity model of the hydrothermal system in Long Valley Caldera, California, from magnetotellurics: Geophysical Research Letters, v. 43, no. 15, p. 7953–7962, https://doi.org/10.1002/2016GL069263.

Schmidt, Kenneth D. and Associates, 2018, Annual report on results of Mammoth Community Water District groundwater monitoring program for October 2016–September 2017: Report prepared for Mammoth Community Water District, Mammoth Lakes, California, 87 p.

Schmidt, Kenneth D. and Associates, 2022, Annual Report on Results of Mammoth Community Water District Groundwater Monitoring Program for October 2020-September 2021. April 2022. https://mcwd.dst.ca.us/wp-content/uploads/2022/04/Mammoth-CWD.pdf

Shevenell, L., Goff, F., Grigsby, C.O., Janik, C.J., Trujillo Jr., P.E., and Counce, D., 1987, Chemical and isotopic characteristics of thermal fluids in the Long Valley Caldera lateral flow system, California: Geothermal Resources Council Transactions, v. 11, p. 195–201, https://www.geothermal-library.org/index.php?mode=pubs&action=view&record=1001612.

Sorey, M.L., 1985, Evolution and present state of the hydrothermal system in Long Valley Caldera: Journal of Geophysical Research, v. 90, no. B13, p. 11219–11228, https://doi.org/10.1029/JB090iB13p11219.

Sorey, M.L., Suemnicht, G.A., Sturchio, N.C., and Nordquist, G.A., 1991, New evidence on the hydrothermal system in Long Valley Caldera, California, from wells, fluid sampling, electrical geophysics, and age determinations of hot-spring deposits: Journal of Volcanology and Geothermal Research, v. 48, p. 229–263, https://doi.org/10.1016/0377-0273(91)90045-2.

Sorey, M.L., Evans, W.C., Kennedy, B.M., Farrar, C.D., Hainsworth, L.J., and Hausback, B., 1998, Carbon dioxide and helium emissions from a reservoir of magmatic gas beneath Mammoth Mountain, California: Journal of Geophysical Research, v, 103, no. B7, p. 15303–15323, https://doi.org/10.1029/98JB01389.

Suemnicht, G.A., and Varga, R.J., 1988, Basement structure and implications for hydrothermal circulation patterns in the western moat of Long Valley Caldera, California: Journal of Geophysical Research, v. 93, no. B11, p. 13191–13207, https://doi.org/10.1029/JB093iB11p13191.

Vaughan, R.G., Bergfeld, D., Evans, W.C., Wilkinson, S., Miwa, C., and Diabat, M., 2018, A baseline thermal infrared survey of ground heating around the Casa Diablo Geothermal Plant, Mammoth Lakes, California: Geothermal Resources Council Transactions, v. 42, p. 962–976, https://www.geothermal-library.org/index.php?mode=pubs&action=view&record=1033957.

White, A.F., and Peterson, M.L., 1991, Chemical equilibrium and mass balance relationships associated with the Long Valley hydrothermal system, California, USA: Journal of Volcanology and Geothermal Research v. 48, p. 283–302, https://doi.org/10.1016/0377-0273(91)90047-4.

White, A.F., Peterson, M.L., Wollenberg, H., and Flexser, S., 1990, Sources and fractionation processes influencing the isotopic distribution of H, O, and C in the Long Valley hydrothermal system, California, USA: Applied Geochemistry, v. 5, p. 571–585.